APOLLO BASIN: A PROBE FOR EARLY LUNAR PROCESSES AND HISTORY Ross W. K. Potter[1,2] and James W. Head[1,2], [1]Department of Earth, Environmental and Planetary Sciences, Brown University, Providence, RI, 02912, USA, [2]NASA Solar System Exploration Research Virtual Institute, ross_potter@brown.edu.

Introduction: The ~500 km diameter pre-Nectarian Apollo peak-ring basin is ideally positioned to investigate early lunar processes and history. Located within the largest lunar basin, South Pole-Aitken (SPA), a synthesis of morphometric, spectroscopic and gravity observations [e.g., 1-5] demonstrates Apollo's distinctive structure. Noritic and basaltic materials are found to the south and west of the basin, while anorthositic materials are found to the north and east [2]. This may be due to Apollo potentially straddling the boundary between SPAs transient crater and modification zone, based on SPA numerical modeling [6]. Apollo's peak-ring rises 1-2 km above the basin's floor; Moon Mineralogy Mapper (M^3) data [3,5] suggests this is dominated by mafic materials. The thin (<5 km) crust beneath the basin center, as well as the possible presence of a SPA melt sheet beneath [5] could also provide mafic signatures. The age, geology and structure of Apollo make it a strong candidate for both robotic and human missions focused on early lunar processes and the structure of the SPA terrane. China has placed Apollo as a top candidate for its 2019 Chang'e-4 landing and roving mission [7].

This work investigates the formation of Apollo using numerical modeling and remote sensing data to understand its unique structure, the structure of SPA and Apollo's importance for future lunar surface missions.

Methods: The iSALE shock physics code [8-10] was used to model the formation of Apollo. Lunar crust and mantle properties were represented by equations of state and strength models for gabbroic anorthosite [11-14] and dunite [13,15,16], respectively. Due to Apollo's unique positioning within SPA, crustal thicknesses of 20 and 40 km were used to represent the differences between the south-west and north-east parts of the basin [17]. A thermal profile with a gradient of 10 K/km and upper mantle temperatures at the solidus [6,18] was used, based on the age and location of Apollo. Impact velocities of 10 and 15 km/s were investigated, along with impactors 32-60 km in diameter. Cell size was nominally 1 km; specific models were run at a higher resolution of 0.5 km per cell. Simulations were carried out in a two-dimensional half-space, with surface gravity set to 1.63 m/s^2.

Results:

Formation. Figure 1 illustrates two Apollo-sized basins, using (a) 40 km and (b) 20 km crusts, after the dynamic phase of basin formation has been completed (~60 minutes after impact). This size of impact (40 km impactor diameter; 15 km/s impactor velocity) excavated material from a maximum depth of ~31 km for both crustal thicknesses. The numerical models, therefore, demonstrate that the Apollo basin-forming impact would have excavated mantle material if crustal thickness was <~30 km. This agrees with previous studies that considered crater scaling laws [5,19,20].

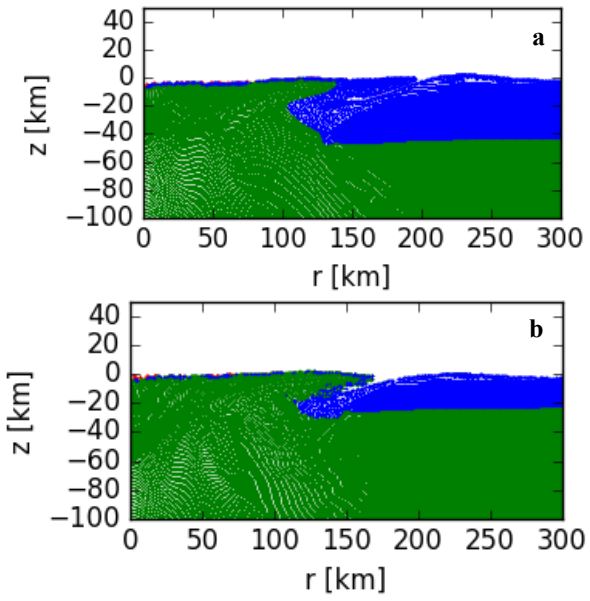

Figure 1. Material distribution (of tracers) for two Apollo-sized basins using crusts (a) 40 km and (b) 20 km thick (red = impactor, blue = crust, green = mantle).

Material distribution. For the 40 km crust scenario, a thin (1-2 km thick) layer of crustal material is present on the basin floor. Some impactor (and mantle) material is mixed in. This material is highly shocked (>35 GPa; Fig. 2a) and melted. These high surface shock pressures continue out to the peak ring (~100-120 km radius). The peak ring consists of crustal material from a variety of depths up to 55 km. Beyond the peak ring, peak shock pressures are lower (<25 GPa); this includes the basin rim material which is composed of crustal material originally from depths <30 km.

For the 20 km crust scenario (Fig. 2b), crustal material is discontinuously found at the basin surface in thin layers (~1-2 km). The peak ring is mainly mantle, consisting of material originally up to 60 km depth. The basin rim consists of crustal material from depths of 5-20 km.

Discussion: M^3 data suggests Apollo's peak ring is dominated by Class C spectra [5] as it contains <95% pure plagioclase and has no clear 1.25 µm plagioclase absorption signature [21]. The 40 km crust numerical models

presented here demonstrate that peak ring material is dominated by anorthosite that experienced peak shock pressures in excess of 35 GPa. This is high enough for plagioclase to lose its 1.25 µm absorption band and, therefore, match the observations. Further M^3 analysis of craters near Apollo's peak ring suggests the presence of Mg-rich material [3], further implying a more mafic composition.

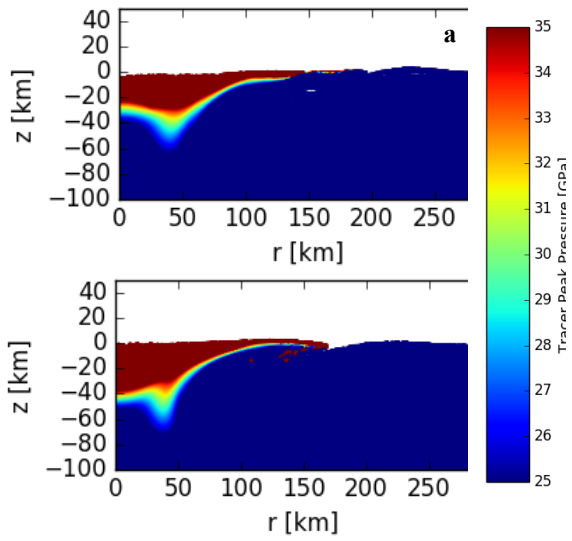

Figure 2. Peak shock pressure distribution for two Apollo-sized basins using crusts (a) 40 km and (b) 20 km thick. Anorthosite in the peak ring is shocked above 25 GPa, thereby losing its crystalline structure.

The mafic dominated composition of Apollo could be due to the magnitude of impact and its location within SPA. Apollo may straddle SPAs transient crater and modification zone [6]. Such positioning means the impact may have occurred into a target dominated by (SPA excavated) upper mantle material, possibly differentiated. Scaling laws suggest excavated material thickness could be up to ~20 km around Apollo's center [22]. The numerical models suggest significant thinning of the crust beneath Apollo to ~1-2 km. Gravity data [4] suggests it could be slightly thicker (~5 km). The crust beneath Apollo, which may have been produced by SPA melt sheet differentiation, is likely to have already been thinned by the SPA impact. Thinner pre-impact crust toward the center of SPA is likely to result in greater mafic content in and around Apollo, as suggested by the 20 km crust scenario numerical model.

Notably, observations at Apollo differ to those at Schrödinger basin, also in SPA. Though Schrödinger is smaller in size (~320 km diameter) and farther (900 km) from SPA's center, olivine exposures have been identified [23]; they have not at Apollo. Schrodinger and Apollo have similar inferred pre-impact crustal thicknesses (25-40) [17], but Schrödinger has a shallower excavation depth (19-24 km) [24]. These observations strongly suggest that SPAs subsurface structure and composition is heterogeneous.

Robotic and/or human missions at Apollo basin would, therefore, represent an excellent opportunity to investigate the likely heterogeneous structure beneath SPA and better understand early lunar history.

Acknowledgements: We gratefully acknowledge the developers of the iSALE shock physics code (www.isale-code.de).

References: [1] Pieters, C. M. et al. (2001) *JGR*, 106, 28001-28022. [2] Petro, N. E. et al. 2010, *LPSC XLI*, #1802. [3] Klima, R. L. et al. (2011) *JGR*, 116, E00G06. [4] Wieczorek, M. A. et al. (2013) *Science*, 339, 671-675. [5] Baker D. M. H. and Head J. W. (2015) *Icarus* 258, 164-180. [6] Potter, R. W. K. et al. (2012) *Icarus*, 220, 730-741. [7] Wang, Q. and Liu, J. (2016) *Acta Astronautica*, 127, 678-683. [8] Amsden, A. A. et al. (1980) Los Alamos National Laboratory Report LA-8095. [9] Collins, G. S. et al. (2004) *MAPS*, 39, 217-231. [10] Wünnemann, K. et al. (2006) *Icarus*, 180, 514-527. [11] Thompson, S. L. and Lauson, H. S. (1972) Sandia National Laboratory Report SC-RR-71 0714. [12] Stesky, R. M. et al. (1974) *Tectonophysics*, 23 177-203. [13] Shimada, M. A. et al. (1983) *Tectonophysics*, 96, 159-172. [14] Azmon, E. (1967) NSL 67-224, 16pp. [15] Benz, W. et al. (1989) *Icarus*, 81, 113-131. [16] Ismail, I. A. H. and Murrell, S. A. F. (1990) *Tectonophysics*, 175, 237-248. [17] Baker, D. M. H. et al. (2013) *LPSC XLIV*, #2662. [18] Potter, R. W. K. et al. (2013) *JGR*, 118, 963-979. [19] Petro, N. E. and Jolliff, B. L. (2013) *LPSC XLIV*, #2724. [20] Morrison, D. A. (1998) *LPSC XXIX*, #1657. [21] Cheek, L. C. et al. (2013) *JGR*, 118, 1805-1820. [22] McGetchin, T. R. et al. (1973) *EPSL*, 20, 226-236. [23] Yamamoto, S. et al. (2012) *Icarus*, 218, 331-344. [24] Kring, D. A. et al. (2016) *Nature Communications*, 7, 13161.